Journal of Materials Chemistry A

Accepted Manuscript

ROYAL SOCIETY OF CHEMISTRY

www.rsc.org/materialsA

Superionic Conduction of Silver in Homogeneous Chalcogenide Glasses

M. Marple, D.C. Kaseman, S. Kim, S. Sen

Dept. of Materials Science & Engineering, University of California at Davis,

Davis, CA 95616, USA

Abstract

Fast ion conducting glasses are of key interest for their potential applications in energy conversion/storage, memory, display and sensor technologies. However, the best contenders in this class of materials suffer from the lack of thermodynamic stability against phase separation, devitrification and moisture attack. We report the finding of novel off-stoichiometric glass-forming chalcogenide alloys in the system Ag-Ga-Ge-Se characterized by modified random networks that overcome these debilitating problems and at the same time display superionic silver conduction at ambient temperature. Combined application of multi-nuclear magnetic resonance, Raman and electrochemical impedance spectroscopy provides a fundamental understanding of the potential energy landscape for silver ion transport in these materials.

▪ Introduction

Inorganic structures that provide suitable pathways for fast ion migration are of particular interest because of their potential application as solid electrolytes in next-generation solid-state energy conversion/storage, switching and sensing devices.[1-6] Inorganic solid electrolytes offer several advantages over more commonly used organic polymer or liquid electrolytes as the latter materials are often fraught with practical problems including relatively poor thermal and chemical stability as well as flammability, and relatively low limit on the operational voltage that restricts their power density when used in batteries.[7,8] Over the years, discovery of considerably high ionic conductivity (e.g. $\geq 10^{-3}$ S/cm at ambient temperature) in numerous crystalline solids that contain mobile cations, has led to extensive studies of the fundamental and application-oriented aspects of cation diffusion in crystalline lattices.[1-5] On the other hand, progress in identifying amorphous materials or glasses with high cation conductivity has suffered from the lack of mechanistic understanding of cation transport in these materials.[9-13] Nevertheless the isotropic nature and the absence of grain boundaries (i.e. interfaces between two neighboring crystallites in polycrystalline solid that often blocks the internal ionic current) in glasses and their compositional flexibility make them highly attractive as solid electrolytes.[9,13] Additionally, the ease in their fabrication/forming ranging from thin films to large shapes and sizes makes glassy materials attractive for various technological applications.[9]

Fast ion-conducting glasses are often found in chalcogenide systems, where conductivity greater than 10^{-4} S/cm around room temperature is abundant for a variety of mobile cations but most notably for Li^+ and Ag^+ in sulfide glasses such as those in Li_2S-SiS_2 and Ag_2S-Ga_2S_3-GeS_2 systems.[14-20] Ag-ion conduction has also been studied extensively in oxide glasses (phosphates, molybdates and borates) and chalcogenide glasses in the Ag_2S-GeS_2-AgI system, all containing

AgI as a major component.[13,17,21-28] However, most of these glasses in the fast ion-conducting regime suffers from the lack of good glass-forming ability (e.g. formation of bulk glasses requires application of rapid melt quenching or adoption of alternative glass-forming routes such as mechanical milling), chemical instability against moisture as well as thermodynamic instability against phase separation.[15,29,30] Therefore the search for chemically stable, single-phase and thermodynamically stable fast ion-conducting glassy electrolytes remains an active area of research. Here we report the finding of novel fast Ag-ion conducting glasses in the ternary system Ag_2Se-Ga_2Se_3-$GeSe_2$ (AGGS) that are thermodynamically stable against crystallization and phase separation, show no degradation from interaction with ambient air and display remarkably large ionic conductivity of ~ $3.2x10^{-4}$ S/cm at room temperature. Glasses in this ternary system were synthesized using the typical melt-quench method. Ideally, glasses with high Ag contents are expected to display high ionic conductivity and such glass compositions would simply lie along the Ag_2Se-$GeSe_2$ join with $GeSe_2$ forming a tetrahedral network and Ag^+ playing the role of modifier cation.[19,20] However, such glasses have been shown in previous studies to have two glass transition temperatures T_g indicative of phase separation with Ag-rich percolating microstructures providing preferred pathways for fast Ag-ion transport. Unfortunately, in spite of their high ionic conductivity, the presence of phase separation renders the ionic transport properties in these glasses strongly dependent on their thermal history. We have found that addition of ≥10 mol% Ga_2Se_3 prevents phase separation in these glasses as they are characterized by a single T_g. Although the composition range for homogeneous glass formation in this ternary system appear to be quite large (details of glass formation range to be published elsewhere), in the present work we primarily focus on glasses with 10 mol% Ga_2Se_3 and with high Ag content (16mol% ≤ Ag_2Se ≤ 40mol%) that are characterized by some of the highest ionic conductivities.

▪ Experimental Section

Synthesis

The AGGS glasses explored in this study are five stoichiometric compositions in the ternary system Ag_2Se-Ga_2Se_3-$GeSe_2$ with 10 mol% Ga_2Se_3 and 16 mol% ≤ Ag_2Se ≤ 40 mol% and two off-stoichiometric compositions with either an excess or deficiency of 5 mol% Se with respect to the base composition of 40%Ag_2Se-10%Ga_2Se_3-50%$GeSe_2$. These glass compositions are listed in Table 1. All AGGS glasses were synthesized from mixtures of Ge (99.9999%), Se (99.999%), and Ag (99.999%) powder and pellets of Ga (99.9999%) using the conventional melt quench method. Batches were sealed in evacuated (~10^{-4} Torr) fused silica ampoules and melted in a rocking furnace by heating to 1050°C at a rate of 100°C/hour, followed by holding at the temperature for 6 hours. Subsequently the melts were cooled to and held at 950°C for 24 hours to ensure homogeneity. The ampoules were then quenched into ice water and glass samples were extracted by fracturing the ampoule. Larger pieces of the bulk glass were polished to obtain parallel surfaces to be used for electrical impedance spectroscopy measurements.

The $AgInSe_2$ and Ag_8GeSe_6 compounds were synthesized via slow cooling of the corresponding melts. In each case mixture of the appropriate amounts of the constituent elements was batched and taken in evacuated quartz ampoule. The batch was slowly heated to 1000°C at a rate of 100°C per hour and the melt was homogenized for 24 to 60 hours in a rocking furnace. In the case of $AgInSe_2$ rocking was stopped and the melt was slowly cooled to 780°C over a period of 4 hours and held at that temperature for another 4 hours. The furnace was then shut off and the ampoule was cooled down to room temperature followed by sample extraction. In the case of

Ag_8GeSe_6 the melt was cooled from 1000°C to 910°C and rocking was ceased. The melt was then cooled to 850°C and held for 24 hours at this temperature before final cooling to room temperature by shutting off the furnace.

Density measurements

Density measurements were carried out using a Micromeritics AccuPyc II gas expansion pycnometer under a helium environment of 6N purity. Approximately 0.5–2.0 g of each sample was loaded into a 1 cm^3 cup. Reported densities are averages of 10 consecutive measurements at 20 °C and are determined to within ±0.005 g/cm^3.

Differential scanning calorimetry (DSC)

Conventional DSC scans were taken using a Mettler-Toledo DSC1 calorimeter. Scans were performed in a flowing nitrogen environment on 15–20 mg of sample loaded into 40 μL aluminum crucibles. The glass transition temperature T_g is determined as the onset of the glass transition region, when heating at a rate of 10 K/min.

NMR spectroscopy

All NMR spectra, unless otherwise noted, were acquired at an external magnetic field of 11.74T using a Bruker magnet and a Bruker Avance500 spectrometer operating at 23.3, 95.4 and 152.5 MHz, respectively, for ^{109}Ag, ^{77}Se and ^{71}Ga. Variable temperature ^{109}Ag static NMR spectra of select AGGS glasses were collected using a low-gamma 4mm probe and a Hahn echo pulse sequence with 170μs delay between the π/2 (9μs) and π (18μs) pulses and a recycle delay of 15s. 150 to 400 free induction decays (FID) were averaged and Fourier transformed to obtain each spectrum. Temperature calibration was performed externally, using the temperature dependence

of the ^{63}Cu isotropic chemical shift of CuBr.[31] The ^{109}Ag static NMR spectrum of the $AgInSe_2$ crystal was acquired with a 19.6T narrow bore magnet equipped with a Bruker DRX console operating at a resonance frequency of 38.7 MHz. All ^{109}Ag spectra were externally referenced to ^{17}O signal of neat, natural abundance H_2O shifted according to the IUPAC recommended frequency reference ratio of 4.653533/13.556457.

The ^{77}Se MAS NMR spectra were collected using a 5mm Doty XC probe. Crushed glass samples were taken in a Si_3N_4 rotor and were spun at 15 kHz. Spectra were collected using a Hahn echo pulse sequence with a rotor synchronized delay between the $\pi/2$ (2.2μs) and π (4.4μs) pulses and a recycle delay of 200s. Approximately 900 FIDs were averaged and Fourier transformed to obtain each spectrum. All ^{77}Se chemical shifts were referenced to the isotropic ^{77}Se chemical shift of crystalline $(NH_4)_2SeO_4$ (δ_{iso}=1040.2ppm).

The high-resolution ^{71}Ga MAS NMR spectra were obtained using the previously described QMAT pulse sequence.[32] Crushed glass samples were taken in a 7mm ZrO_2 rotor and were spun at 7 kHz. QMAT is a two dimensional NMR spectroscopic technique that uses linearly varying delays between ten central transition selective pulses to yield an "infinite spinning speed" MAS spectrum. The central transition selective $\pi/2$ and π pulse lengths were 1.3 and 2.6μs, respectively, with a 112 kHz radio frequency field. A total of 16 t_1 increments were employed over a single rotor period. 10000 transients were collected for each t_1 slice using a 0.2s relaxation delay between each transient allowing a full 2D spectrum to be acquired in under 10 hours. The "infinite spinning speed" MAS spectra are obtained through summation of the 16 t_1 increments after shearing and Fourier transforming both direct and indirect dimensions. All ^{71}Ga chemical shifts were referenced to the isotropic chemical shift of 1M $Ga(NO_3)_3$ (δ_{iso}=0 ppm).

Raman Spectroscopy

The ambient temperature unpolarized Raman spectra of the AGGS glasses were collected using a Bruker RFS 100/S Fourier-transform Raman spectrometer equipped with a Nd:YAG laser operating at 1064 nm in the backscattering geometry. The power level and the resolution were set to 30 mW and 2 cm^{-1}, respectively.

Electrical Impedance spectroscopy

The conductivity of these glasses was measured using a HP 4192A LF Impedance Analyzer. Polished pieces of glass with two parallel surfaces were used. Platinum electrodes were sputtered on the parallel surfaces. Electrical measurements were carried out between room temperature and 100°C. Conductivity σ is computed using the equation, $\sigma = R^{-1}(L/A)$ with A and L being the area of the electrodes and the distance between them, respectively. Resistance, R, of the individual samples is determined by comparing the complex impedance of the samples measured over a wide range of frequencies (5Hz to 13MHz) at a given temperature to those simulated using an appropriate equivalent circuit that retains the electrical characteristics of the samples. The equivalent circuit used is composed of a parallel RQ circuit, where R is a resistor and Q is a constant phase element. The dielectric constant ε_r is calculated from the simulated Cole-Cole plot of complex impedance by converting the constant phase element to a capacitor using the expression $C = (TR^{1-p})^{1/p}$ where T and p are the fitting parameters for a constant phase element of impedance $Z = \frac{1}{T(i\omega)^p}$. The dielectric constant is then found from the expression for parallel plate capacitance, $C = \varepsilon_r \varepsilon_0 \frac{A}{L}$.

Transference Number Measurement

Ag ion transference number t_i, i.e. the ratio of ionic conductivity to total conductivity, for the stoichiometric and off-stoichiometric AGGS glasses with the highest electrical conductivities was measured using the electromotive force (EMF) method. The transference number t_i was determined by measuring the open circuit voltage (OCV) developed within a galvanic cell, and comparing the theoretical value of the equilibrium potential of the formation reaction E_{th} with the measured value E_m and using the relation $E_m = t_i E_{th}$. In this study the solid state galvanic cell used was Ag|AGGS glass|Se,C. The Se,C electrode was prepared by adding 25 weight % graphite powder to amorphous Se to make the latter electrically conductive. To ensure good contact between the glass electrolyte and Se,C electrode, powdered layers were pressed at 6 MPa into single pellets using a hydraulic press. Ag foil was used as the Ag electrode and the entire cell assembly was pressed together between Pt electrodes under spring tension to ensure good contact between the Ag foil and the glass electrolyte. The free energy of formation ΔG_f for the cell reaction: $2Ag(s) + Se(s) \leftrightarrow Ag_2Se(s)$ can be used to determine the EMF of the cell through the Nernst equation, $\Delta G_f = -nFE_{th}$, where n is the number of electrons in the reaction, F is the Faraday constant, and E_{th} is the equilibrium potential of the formation reaction. This yields a room temperature value of $E_{th} = 244$ mV.[33] The OCV was measured using a Keithley 617 electrometer with input impedance greater than 10^{14} Ohms. Each EMF value E_m was taken after its stabilization to within ±0.5 mV for a few hours.

▪ Results and Discussion

The density and T_g of the AGGS glasses with 10% Ga_2Se_3 are listed in Table 1. For stoichiometric compositions the density increases and T_g decreases monotonically with increasing Ag_2Se concentration. These results are consistent with the replacement of Ge with more massive

Ag in the structure of these glasses and the concomitant loss of connectivity of the predominantly corner-shared network of $GeSe_4$ tetrahedra upon incorporation of the modifier Ag_2Se (*vide infra*). Moreover, all homogeneous glasses are characterized by a single glass transition, indicating the absence of phase separation at any significant length scale (see Fig. 1). As the extent of phase separation in these glasses is difficult to determine, here we use the criterion that glasses that lack a detectable second glass transition are homogeneous.

The ^{71}Ga, ^{77}Se and ^{109}Ag NMR spectra of the AGGS glasses are shown in Fig. 2. The ^{71}Ga NMR spectra of all glasses are characterized by a single asymmetric peak with a low-frequency tail characteristic of quadrupolar nuclides with a distribution of quadrupolar coupling constants associated with site disorder typical of glassy materials (Fig. 2a). The peak position is consistent with Ga in tetrahedral coordination with Se atoms in $GaSe_4$ tetrahdera.[34] Similarly the ^{77}Se NMR spectra of these glasses consist of a main peak centered at ~ 394 ppm, characteristic of two-coordinated Se sites corner-shared by $(Ge,Ga)Se_4$ tetrahedra (Fig. 1b).[34] Increasing Ag content results in the appearance of additional intensity in these ^{77}Se NMR spectra in the region between ~ 250 and –250 ppm (Fig. 2b). A comparison with the ^{77}Se NMR spectrum of the model compound Ag_8GeSe_6 suggests that these additional peaks correspond to non-bridging Se atoms in the glass structure that are bonded to only 1 Ge atom and several Ag atoms (Fig. 1b). This result indicates that Ag plays the classic role of a network modifier in the structure of these glasses as its addition results in breaking up of the $(Ga,Ge)Se_4$ tetrahedral network with the formation of non-bridging Se atoms. Finally, a comparison of the ^{109}Ag NMR spectra of these glasses with that of the $AgInSe_2$ model compound (Fig. 2c) indicates that Ag atoms are likely to be higher than fourfold coordinated in the glass structure. Future studies will be required to determine a chemical shift scale to quantitatively determine the coordination number of Ag atoms in these glasses. However,

a higher than fourfold coordination environment for Ag is consistent with its role as a classical network modifier. When taken together, the analyses of these multinuclear NMR spectra shed light on the structural details of these glasses in a comprehensive fashion. The atomic structure of these AGGS glasses can be described as a network of corner- and edge-sharing $(Ge,Ga)Se_4$ tetrahedra where the introduction of Ag as Ag_2Se results in the breakdown of the connectivity of the network via formation of non-bridging Se atoms.[19]

This structural scenario for the AGGS glasses is consistent with the Raman spectroscopic results presented in Fig. 3. The Raman spectra of these glasses are dominated by a strong peak near ~200 cm^{-1} corresponding to the (Ga,Ge)-Se stretching mode of corner-shared $(Ge,Ga)Se_4$ tetrahedra while the tetrahedral bending modes can be observed in the low frequency region between 80 and 130 cm^{-1}. Finally, the Raman spectra of all glasses display a band near ~250 cm^{-1}, corresponding to Se-Se stretches, implying a violation of chemical order (Fig. 3). This band sharply drops in intensity with increasing Se deficiency in off-stoichiometric glasses indicating a decrease in the fraction of low-dimensional Se-Se linkages. This structural change is manifested in the concomitant marked increase in density and T_g of the 5% Se-deficient glass compared to its stoichiometric counterpart (Table 1).

The electrical characteristics of these AGGS glasses with various Ag contents as obtained from the results of ac-impedance spectroscopy are listed in Table 1 and the Arrhenius plots of the conductivity σ of each of the samples is shown in Fig. 4. The σ of all AGGS glasses under investigation follows an Arrhenius behavior, which we attribute to thermally activated hopping of Ag^+ in them. The glass composition $40Ag_2Se$-$10Ga_2Se_3$-$50GeSe_2$ displays the highest room-temperature conductivity (10^{-4} S/cm) among all stoichiometric compositions which can be further tuned by compositional engineering of the Se content (Fig. 4). Addition of Se to the glass of

composition $40Ag_2Se$-$10Ga_2Se_3$-$50GeSe_2$ by 5% above stoichiometry results in a marginal increase in σ (~20%) while the latter is maximized to a value of ~ $3.2x10^{-4}$ S/cm at room temperature in the same base glass when it is deficient in Se by 5% (Fig. 4). Further increase in Se deficiency results in phase separation as evidenced by the appearance of two T_g in their DSC scans. This maximum value of σ in a homogeneous AGGS glass is an order of magnitude higher than that ($2.5x10^{-5}$ S/cm) for a glass of similar composition in the corresponding sulfide system ($46Ag_2S$-$8Ga_2S_3$-$46GeS_2$) reported in a previous study.[16]

Previous studies of Ag containing sulfide and selenide glasses indicated that the σ in these glasses was predominantly ionic in nature with Ag-ion transference number approaching ~1 for Ag ion concentration ≥ 0.5 at%.[16, 19] The EMF measurements carried out in this study on AGGS glasses are in complete agreement with these previous results. The measured EMF values for the stoichiometric AGGS glasses with 30 and 40 mol% Ag_2Se are 237 and 230 mV, respectively, while that for the 40 mol% Ag_2Se off-stoichiometric glass with 5% Se-deficiency is 235 mV, leading to transference numbers greater than 0.94 in all cases. These experiments provide unequivocal proof that the σ in these glasses originate predominantly from fast Ag ion conduction. Furthermore, direct temperature dependent ^{109}Ag NMR line shape analyses of these glasses corroborates this hypothesis. The ^{109}Ag NMR line widths for the stoichiometric glasses with 30 and 40 mol% Ag_2Se and the off-stoichiometric Se-deficient glass with 40 mol% Ag_2Se are shown in Fig. 5 over temperatures ranging between 0 °C and 175 °C. The temperature dependence of the ^{109}Ag NMR line width directly implies fast Ag ion motion even at room temperature (Fig. 5). In the case of motional narrowing of the NMR line width for a spin-1/2 nuclides such as ^{109}Ag, identical NMR line widths for different but related materials must correspond to similar diffusivity of Ag ions and hence, to similar ionic conductivity. As can be seen in Fig. 5, identical ^{109}Ag NMR

line widths for the stoichiometric and Se-deficient AGGS glasses with 40 mol% Ag_2Se are shifted in the temperature scale by ~30 °C in the region between the rigid lattice and motionally narrowed regimes. This temperature shift is similar to the value expected from the temperature dependence of the σ of these two samples (Fig. 4) indicating that the latter is indeed controlled by Ag ion conduction in these materials.

We note that the σ is highly sensitive to the Ag content in these AGGS glasses, it enhances by more than 4 orders of magnitude as the Ag content increases only by a factor of 2.5 (from 16 to 40 mol% or equivalently from 10 to 25 atom%). Since electrical conductivity is linearly dependent on the product of number density of mobile ions and their mobility, it is clear that the rapid increase in σ with Ag concentration must originate from increasing mobility of Ag^+ in the structure of AGGS glasses. Mobility is exponentially dependent on the activation energy for ionic hopping and indeed the activation energy E_a for the Ag^+- hopping in AGGS glasses reduces sharply from 0.54 to 0.31 eV with increasing Ag concentration (Table 1). These remarkable changes in the electrical characteristics of AGGS with Ag content can be clearly seen in Figs. 4 and 5b. In particular, the strongly non-linear dependence of E_a on Ag concentration for the AGGS glasses is shown in Fig. 5b.

The intrinsic activation energy barrier for ionic hopping at the dilute limit can be described well within the framework of the Andersen-Stuart model where the activation energy depends on the size of the mobile ion, the dielectric constant of the host structure and the shear modulus.[35] The dielectric constants of the AGGS glasses as derived from the impedance spectroscopic measurements are found to vary over a narrow range of 32-40 (Table 1). The T_g values for these glasses also vary over a small range of 212-250 ºC (Table 1) which implies a correspondingly small variation in their shear moduli. Therefore, the observed compositional variation of E_a in

these glasses suggests an effective lowering of the intrinsic activation energy barrier with increasing Ag concentration. The dynamical percolation model of Bunde and coworkers predicts a power-law type decrease in E_a with increasing mobile ion concentration.[36] However, such power-law dependence has been shown in the literature to be valid only over a limited composition range.[19] Furthermore, percolation is not likely to be a controlling factor for ionic transport in glasses with relatively high Ag concentration (10 to 25 atom%). Rather, the progressive depolymerization of the tetrahedral structural network by addition of Ag as a modifier cation must play an important role in controlling the E_a.[19] Such modification of the glass network is expected to result in increasing number of sites where Ag atoms can reside and hop into, when activated.

In this potential energy landscape the effective activation energy barrier for inter-site hopping will be lowered with respect to the intrinsic barrier due to spatial overlap of potential energy wells, as more sites are created with increasing Ag concentration and modification of the network (Fig. 6).[37] The extent of this lowering of hopping energy barrier with respect to the intrinsic barrier at the dilute limit (i.e. zero overlap) depends upon the spatial separation r of the Ag sites or energy wells as well as the shape of the wells (Fig. 6). Although the variation of r with Ag concentration is not known a priori, it is reasonable to assume that r is linearly related to the average Ag-Ag atomic separation $r_{Ag\text{-}Ag}$ in the glass structure. Previous studies have shown that for overlapping potential energy wells defined by Coulombic interaction between an ion and its oppositely charged surrounding, the effective barrier height E_a is lowered with respect to the intrinsic barrier E such that $(E - E_a) \sim 1/r$.[37] As mentioned above, $r_{Ag\text{-}Ag}$ can be used as a proxy for r within a constant factor such that $(E - E_a) \sim 1/ r_{Ag\text{-}Ag}$ or, more generally: $(E - E_a) = C/ (r_{Ag\text{-}Ag})^x$ where C is a constant that incorporates the dielectric constant of the medium and x is a constant that is related to the shape of the potential wells and can be somewhat higher or lower than 1. We have tested the

validity of this scaling relationship by fitting the E_a vs. $r_{Ag\text{-}Ag}$ data for the AGGS glasses in Fig. 5b using this equation where C and x are treated as fit parameters and $r_{Ag\text{-}Ag}$ for different AGGS glasses was obtained from measured densities under the assumption of a random distribution of Ag atoms in the glass structure (Table 1). The value of the intrinsic barrier E was constrained to 0.9 eV which is the activation energy for Ag ion conduction in a variety of chalcogenide glass systems at the dilute limit of Ag concentration (≤ 1 atom%). It is clear that not just the data for the AGGS glasses but previously published activation energy data on Ag-Ge-S glasses over a wide range of Ag concentrations[18] can be successfully described using this type of scaling relationship. Hence, progressive modification of the potential energy landscape for mobile ion hopping is the key factor that controls the mobility of the ions and consequently the resulting electrical conductivity.

▪ Conclusions

Homogeneous and stable, on and off –stoichiometric glasses are synthesized in the Ag-Ga-Ge-Se system. Phase separation in these AGGS glasses can be successfully suppressed by the addition of Ga. Structural characterization using multinuclear NMR spectroscopy suggests that the addition of Ag results in the formation of non-bridging Se atoms and consequent depolymerization of the network of corner and edge -sharing $(Ge,Ga)Se_4$ tetrahedra. This progressive modification of the glassy network results in fast Ag ion conduction in these materials even at ambient temperature. The finding of off-stoichiometric chalcogenide glassy alloys with modified random network characterized by superior thermodynamic stability and fast Ag ion conduction presents exciting new opportunities in developing a novel class of amorphous materials for their application in a wide range of energy and sensing technologies.

Acknowledgements

This work was supported by a grant from the National Science Foundation (NSF-DMR 1104869) to SS.

References:

1. M. Armand and J. M. Tarascon, *Nature*, 2008, **451**, 652-657.
2. J. B. Goodenough and Y. Kim, *Chemistry of Materials*, 2010, **22**, 587-603.
3. E. Quartarone and P. Mustarelli, *Chemical Society Reviews*, 2011, **40**, 2525-2540.
4. J. Maier, *Nature Materials*, 2005, **4**, 805-815.
5. B. Keimer, J. Maier and J. Mannhart, *Nature Materials*, 2012, **11**, 751-752.
6. Y. Sadaoka, Y. Sakai, M. Matsumoto and T. Manabe, *Journal of Materials Science* 1993, **28**, 5783-5792.
7. N. Kamaya, K. Homma, Y. Yamakawa, M. Hirayama, R. Kanno, M. Yonemura, T. Kamiyama, Y. Kato, S. Hama, K. Kawamoto and A. Mitsui, *Nature Materials*, 2011, **10**, 682-686.
8. S. K. Kim, A. Mao, S. Sen and S. Kim, *Chemistry of Materials*, 2014, **26**, 5695-5699.
9. V. K. Deshpande, *IOP Conference Series: Materials Science and Engineering*, 2009, **2**, 012011.
10. T. Minami, A. Hayashi and M. Tatsumisago, *Solid State Ionics*, 2006, **177**, 2715-2720.
11. W. Yao and S. Martin, *Solid State Ionics*, 2008, **178**, 1777-1784.
12. J. Kincs and S. W. Martin, *Physical Review Letters*, 1996, **76**, 70-73.
13. M. Tatsumisago and A. Hayashi, in *Encyclopedia of Applied Electrochemistry*, eds. G. Kreysa, K.-i. Ota and R. F. Savinell, Springer, New York, 2014, DOI: 10.1007/978-1-4419-6996-5, pp. 946-950.
14. S. Kondo, K. Takada and Y. Yamamura, *Solid State Ionics*, 1992, **53**, 1183-1186.
15. P. Boolchand and W. J. Bresser, *Nature*, 2001, **410**, 1070-1073.
16. N. Chbani, A. Ferhat, A. Loireau-Lozac'h and J. Dugué, *Journal of Non-Crystalline Solids*, 1998, **231**, 251-256.
17. E. Robinel, B. Carette and M. Ribes, *Journal of Non-Crystalline Solids*, 1983, **57**, 49-58.
18. E. Bychkov, V. Tsegelnik, Y. Vlasov, A. Pradel and M. Ribes, *Journal of Non-Crystalline Solids*, 1996, **208**, 1-20.
19. E. Bychkov, *Solid State Ionics*, 2009, **180**, 510-516.
20. M. Kawasaki, J. Kawamura, Y. Nakamura and M. Aniya, *Solid State Ionics*, 1999, **123**, 259-269.
21. J. Ren and H. Eckert, *The Journal of Physical Chemistry C*, 2013, **117**, 24746-24751.
22. C. Tomasi, P. Mustarelli, M. P. Infante Garcia, A. Magistris and A. Mandanici, *Philosophical Magazine Part B*, 2002, **82**, 475-483.
23. M. Cutroni and A. Mandanici, *Solid State Ionics*, 1998, **105**, 149-157.
24. S. Bhattacharya and A. Ghosh, *Journal of Physics: Condensed Matter*, 2005, **17**, 5655-5662.
25. P. Mustarelli, C. Tomasi and A. Magistris, *The Journal of Physical Chemistry. B*, 2005, **109**, 17417-17421.
26. J. Kawamura and M. Shimoji, *Journal of Non-Crystalline Solids*, 1986, **88**, 281-294.
27. G. Chiodelli, G. Campari Viganŏ, G. Flor and A. Magistris, *Solid State Ionics*, 1983, **8**, 311-318.
28. T. Minami, Y. Takuma and M. Tanaka, *Journal of the Electrochemical Society*, 1977, **124**, 1659-1662.

29. A. Hayashi, S. Hama, H. Morimoto, M. Tatsumisago and T. Minami, *Journal of the American Ceramic Society*, 2001, **84**, 477-479.
30. M. Tatsumisago and T. Minami, *Materials Chemistry and Physics*, 1987, **18**, 1-17.
31. J. Wu, N. Kim and J. F. Stebbins, *Solid State Nuclear Magnetic Resonance*, 2011, **40**, 45-50.
32. I. Hung and Z. Gan, *Chemical Physics Letters*, 2010, **496**, 162-166.
33. Å. Olin, B. Noläng, E. G. Osadchii, L.-O. Öhman and E. Rosén, eds., *Chemical Thermodynamics of Selenium*, Elsevier, Amsterdam, 2005.
34. A. W. Mao, D. C. Kaseman, I. Hung, Z. Gan, B. G. Aitken and S. Sen, *Journal of Non-Crystalline Solids*, 2015, **410**, 14-19.
35. O. L. Anderson and D. A. Stuart, *Journal of the American Ceramic Society*, 1954, **37**, 573-580.
36. A. Bunde, M. Ingram and P. Maass, *Journal of Non-Crystalline Solids*, 1994, **172-174**, 1222-1236.
37. G. E. Pike, *Physical Review B*, 1972, **6**, 1572-1580.

Table 1: Summary of electrical and physical properties of AGGS glasses with 10% Ga_2Se_3 and varying Ag_2Se content.

mol% Ag_2Se	σ_{RT} (Ω^{-1} cm^{-1})*	E_a (eV)	T_g (°C)	Density (g cm^{-3})	Ag-Ag Separation Distance (Å)	Dielectric Constant (±4)
16	3.40×10^{-9}	0.54	232	4.9335	5.43	40
22	2.76×10^{-7}	0.51	239	5.0759	4.86	34
26	7.80×10^{-7}	0.49	234	5.2142	4.57	33
30	5.16×10^{-6}	0.46	217	5.3452	4.34	33
40	9.36×10^{-5}	0.31	215	5.5015	3.94	38
40 (+5%Se)	1.08×10^{-4}	0.31	212	5.7772	3.87	32
40 (–5%Se)	2.57×10^{-4}	0.32	250	5.8434	3.86	30

*σ_{RT} represents electrical conductivity at ambient temperature.

Figure1.

Figure 1. Representative DSC scans typical of homogeneous AGGS glasses showing a single glass transition for the stoichiometric AGGS glass of composition 40%Ag_2Se-10%Ga_2Se_3-50%$GeSe_2$ (red curve) and for glasses that are off-stoichiometric from this composition with 5 mol% Se excess (green curve) or Se deficiency (blue curve). Also shown for comparison the DSC curve of a phase separated AGGS glass of composition 10%Ag_2Se-40%Ga_2Se_3-50%$GeSe_2$ that displays two glass transitions (black curve). The locations of glass transition and the corresponding T_g values are also shown.

Figure 2.

(a) Representative ^{71}Ga QMAT NMR spectrum of AGGS glass (top: blue solid line) compared with the ^{71}Ga MAS NMR spectrum of crystalline Ga_2Se_3 (bottom: black solid line). Similar isotropic shifts suggest that Ga atoms in AGGS glass are tetrahedrally coordinated to Se.[34] Red dashed line is a simulation of the glass spectrum using the Czjeck model that yields an average quadrupolar coupling constant of ~5.2 MHz and an isotropic shift of ~140 ppm.

(b) ^{77}Se MAS NMR spectra of crystalline Ag_8GeSe_6 (top) and of stoichiometric AGGS glasses (bottom) with different Ag contents. Glass spectra in red, blue, green and pink correspond to samples with Ag_2Se contents of 16, 26, 40 and 40(–5% Se) mol%, respectively. Asterisks in the top spectrum denote spinning sidebands. The crystal structure of Ag_8GeSe_6 consists of two basic types of Se environments in 2:1 ratio: the non-bridging Se atoms that are bonded to 1 Ge and several Ag atoms and Se atoms that are solely bonded to Ag atoms. Integration of peak areas and corresponding chemical shift ranges suggest that the group of high frequency resonances between –150 and 250 ppm in the ^{77}Se MAS NMR spectrum of this crystal correspond to the non-bridging Se environments, while those in the low-frequency region between –700 and –1250 ppm can be

associated with Se atoms bonded to Ag only. The rising intensity in the ^{77}Se MAS NMR spectra of stoichiometric AGGS glasses in the region between −250 and 250 ppm with increasing Ag concentration can therefore be attributed to the progressive modification of the structural network via formation of non-bridging Se atoms.

(c) ^{109}Ag static NMR spectra of crystalline $AgInSe_2$ (red) and of the stoichiometric AGGS glass with 40 mol% Ag_2Se (black) at ambient temperature. The ^{109}Ag NMR spectra of AGGS glasses are found to be practically independent of the chemical composition. The crystal structure of $AgInSe_2$ is characterized by a single Ag site in tetrahedral coordination with 4 Se nearest neighbors. Therefore, the ^{109}Ag resonance in the crystal spectrum near ~1200 ppm can be readily assigned to Ag in fourfold coordination. Consequently, the ^{109}Ag resonance near 900 ppm in the spectra of AGGS glasses is likely indicative of Ag atoms in higher than fourfold coordination. A more quantitative analyses of the coordination number of Ag in these glasses requires further studies towards the establishment of the ^{109}Ag NMR chemical shift scale in selenides.

Figure 3.

Unpolarized Raman spectra of stoichiometric and off-stoichiometric AGGS glasses. The Ag_2Se content and the deviation in the Se content from stoichiometry are given in mol% alongside each spectrum. Vertical dashed lines denote the vibrational bands corresponding to the stretching mode of corner-sharing $(Ga,Ge)Se_4$ tetrahedra and Se-Se linkages. Green and red circles denote Ga/Ge and Se atoms, respectively, in the cartoons of these structural units

Figure 4.

Arrhenius plot of the temperature dependence of electrical conductivity for the stoichiometric and off-stoichiometric AGGS glasses. The Ag_2Se content and the deviation in the Se content from stoichiometry for these glasses are given in mol% alongside the symbols in the legend. Inset shows room-temperature electrical conductivity as a function of Ag_2Se content for the stoichiometric (filled squares) and off-stoichiometric (circle and triangle for the Se-excess and Se-deficient compositions, respectively) AGGS glasses.

Figure 5.

(a) Temperature dependence of ^{109}Ag static NMR spectral line width (full width at half maximum) for the stoichiometric AGGS glass with 30 and 40 mol% Ag_2Se (triangles and circles, respectively) and the off-stoichiometric Se-deficient AGGS glass with 40 mol% Ag_2Se (squares). Inset shows the ^{109}Ag static NMR spectral line shapes for the off-stoichiometric Se-deficient AGGS glass with 40 mol% Ag_2Se, at various temperatures denoted alongside the spectra.

(b) Activation energy of electrical conductivity for the stoichiometric (squares) and off-stoichiometric (circle and triangle for Se-excess and Se-deficient) AGGS glasses as a function of the Ag_2Se content. Inset shows the dependence of the activation energy of electrical conductivity on the average Ag-Ag atomic separation $r_{Ag\text{-}Ag}$ in the glass structure for AGGS glasses studied here (filled circles) and for Ag-Ge-S glasses (open circles) reported in a previous study.[18] The line through the data points is a fit of the potential energy barrier overlap model proposed in the present study using the fitting parameters C = 1.345, x = 0.6, and E = 0.9 eV.

Figure 6.

Lowering of the effective barrier height, E_a, from intrinsic value, E, by overlap of potential wells as distance between Ag sites $r_{Ag\text{-}Ag}$ decreases from left to right.

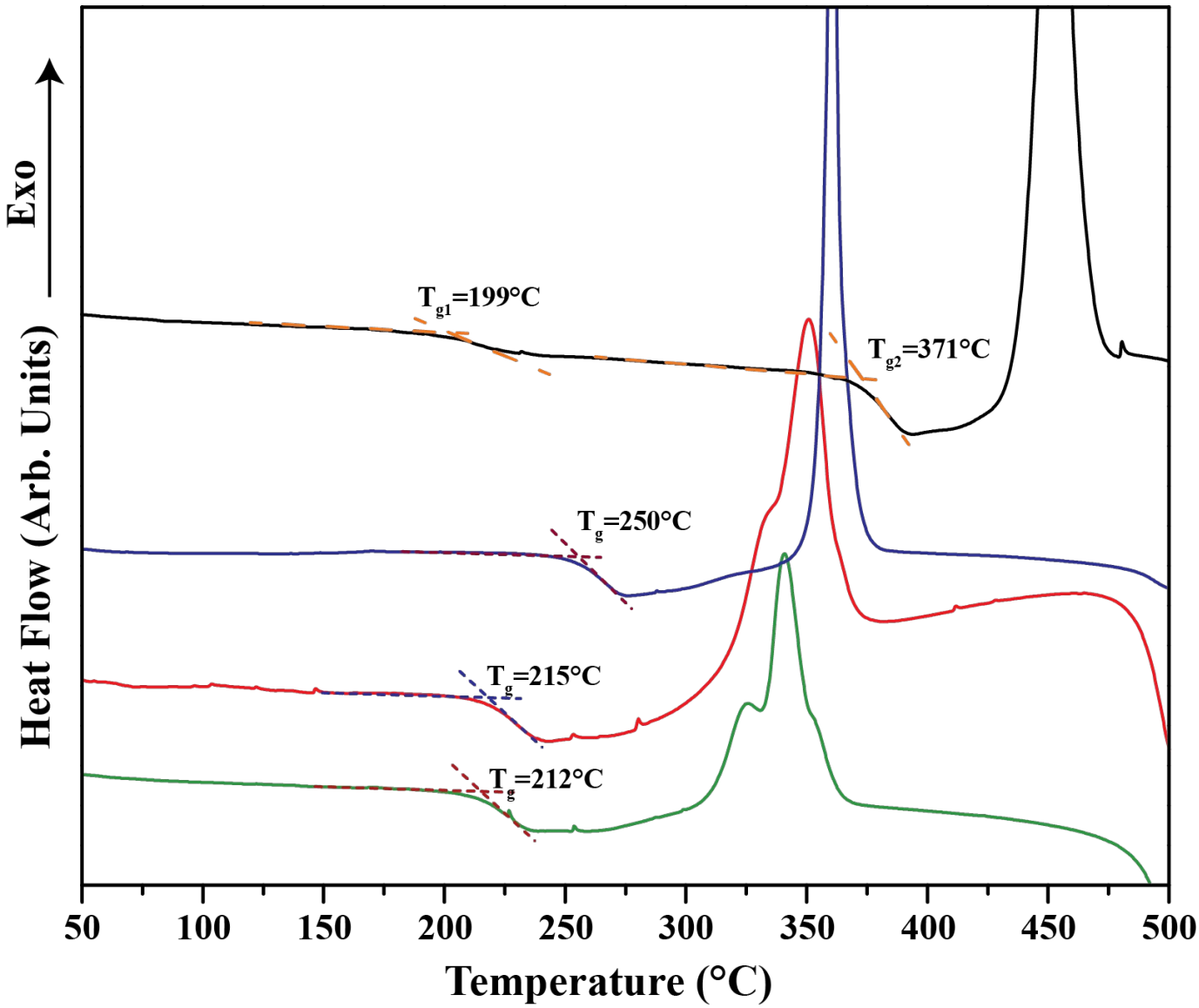

Fig. 1

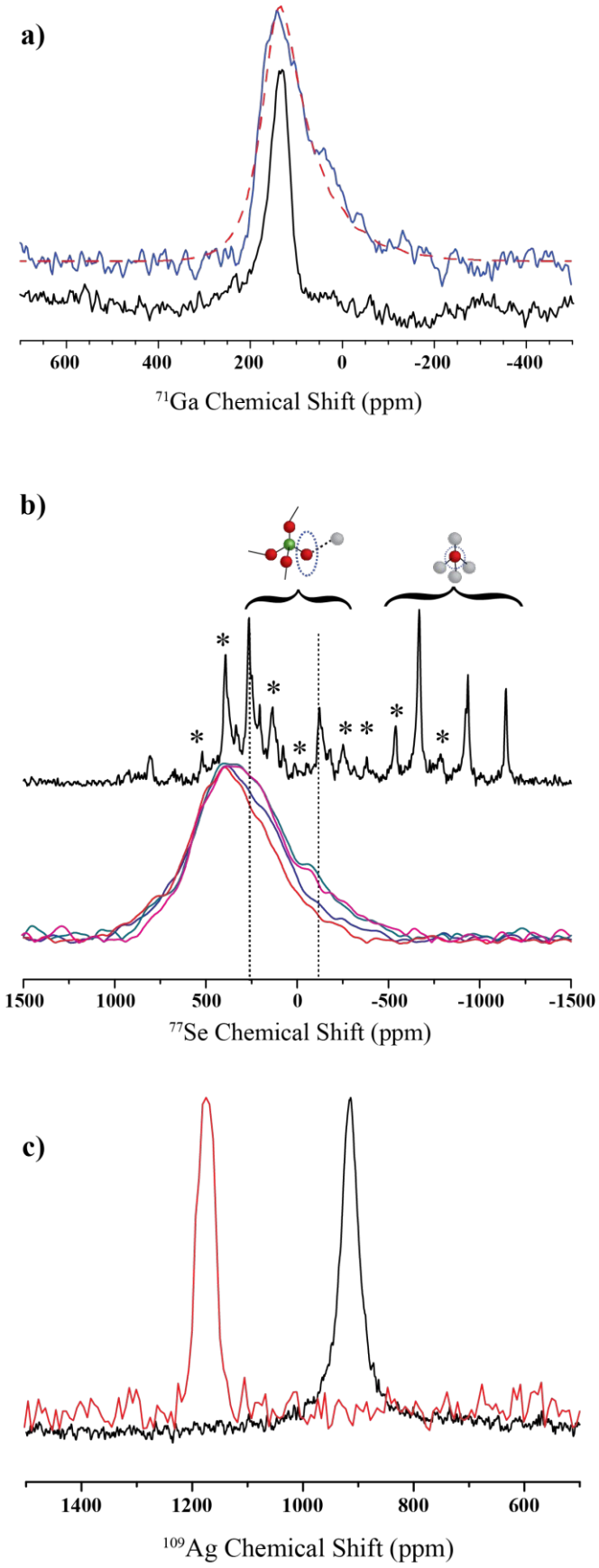

Fig. 2

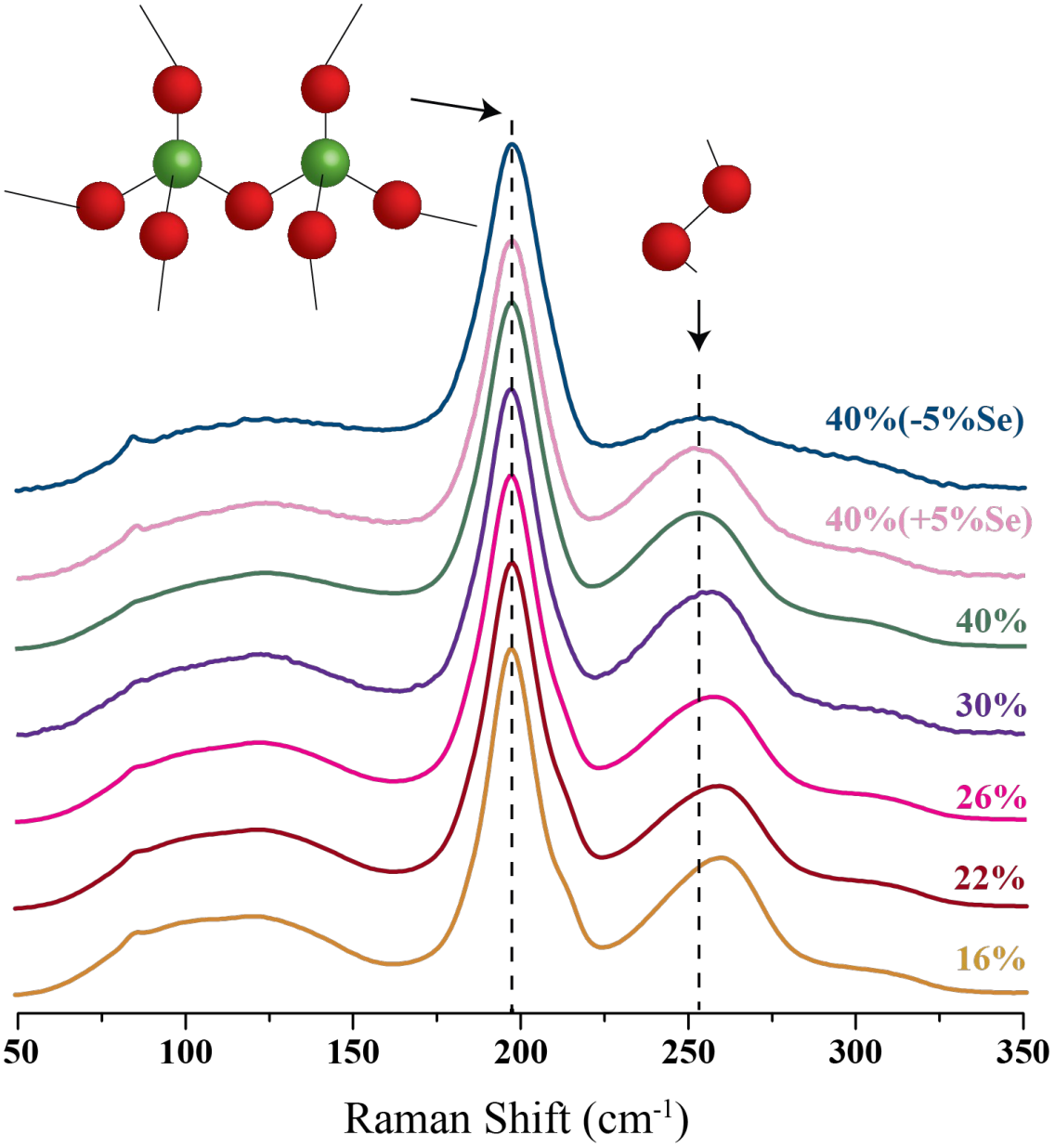

Fig. 3

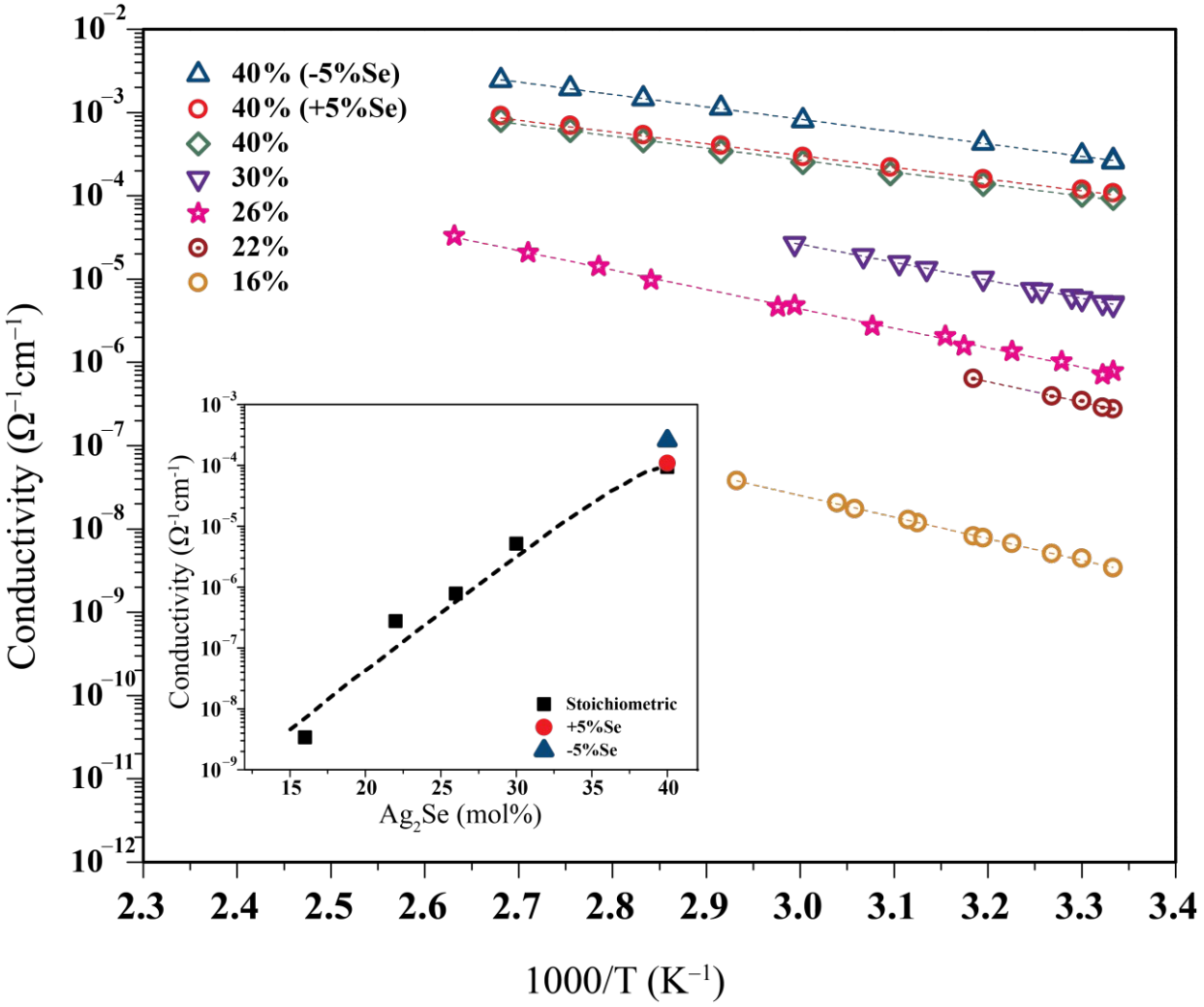

Fig. 4

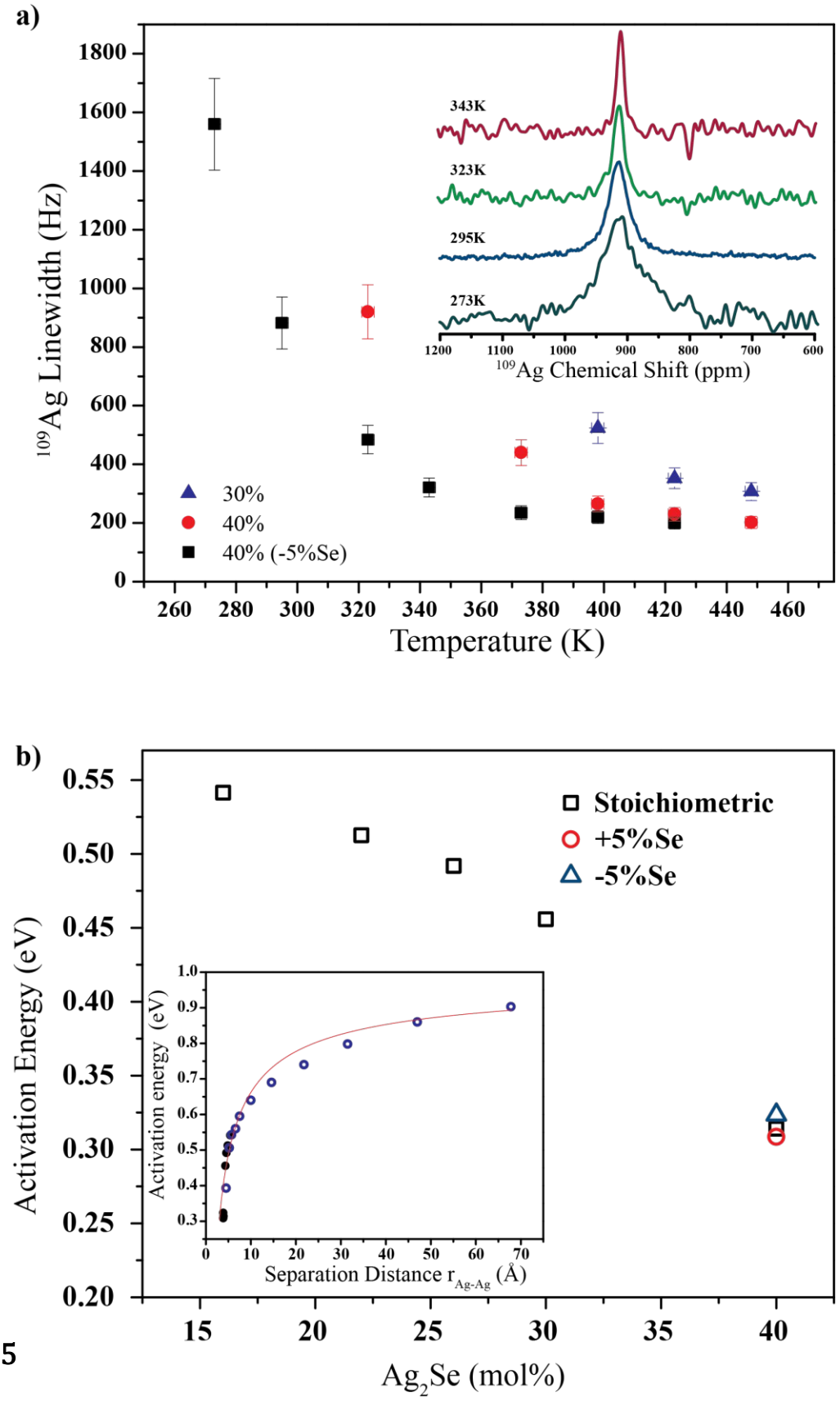

Fig. 5

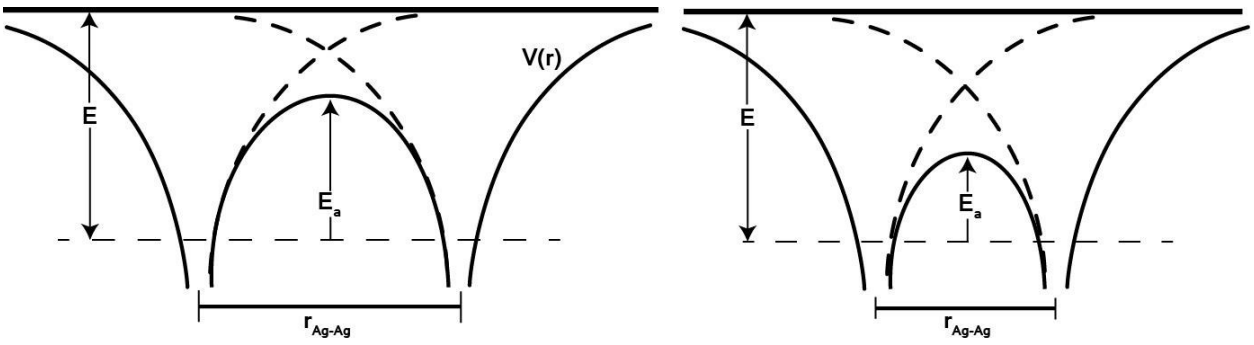

Fig. 6

Table of Contents- Graphics

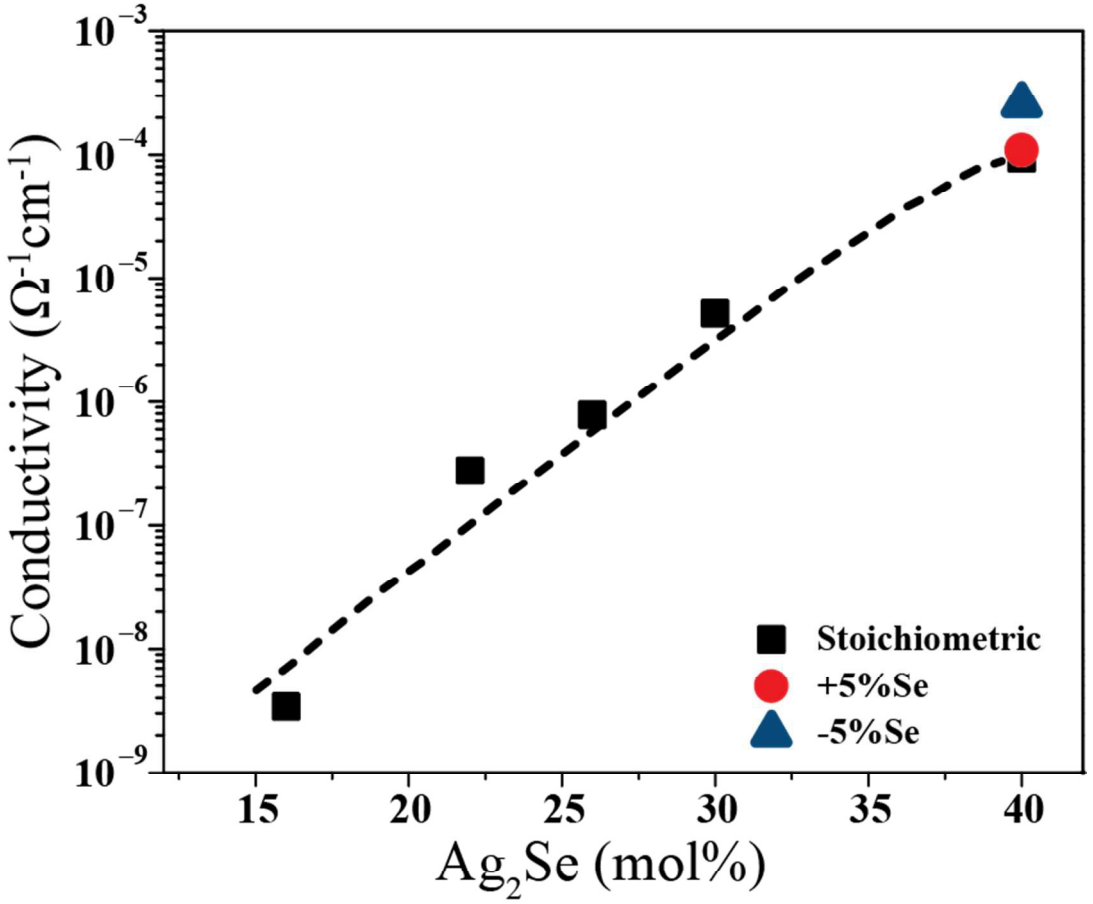

Homogeneous Ag-Ga-Ge selenide glasses display fast silver ion conduction at ambient temperature.